



<b>Publication Year</b>	2014
<b>Acceptance in OA</b>	2024-02-20T13:06:29Z
<b>Title</b>	Baseline design of the thermal blocking filters for the X-IFU detector on board ATHENA
<b>Authors</b>	BARBERA, Marco, COLLURA, Alfonso, Gatti, F., LO CICERO, UGO, MACCULI, CLAUDIO, PIRO, LUIGI, Renotte, E., SCIORTINO, Salvatore
<b>Publisher's version (DOI)</b>	10.1117/12.2057403
<b>Handle</b>	<a href="http://hdl.handle.net/20.500.12386/34792">http://hdl.handle.net/20.500.12386/34792</a>
<b>Serie</b>	PROCEEDINGS OF SPIE
<b>Volume</b>	9144

# PROCEEDINGS OF SPIE

[SPIDigitalLibrary.org/conference-proceedings-of-spie](https://spiedigitallibrary.org/conference-proceedings-of-spie)

## Baseline design of the thermal blocking filters for the X-IFU detector on board ATHENA

M. Barbera, A. Collura, F. Gatti, U. Lo Cicero, C. Macculi, et al.

M. Barbera, A. Collura, F. Gatti, U. Lo Cicero, C. Macculi, L. Piro, E. Renotte, S. Sciortino, "Baseline design of the thermal blocking filters for the X-IFU detector on board ATHENA," Proc. SPIE 9144, Space Telescopes and Instrumentation 2014: Ultraviolet to Gamma Ray, 91445U (25 July 2014); doi: 10.1117/12.2057403

**SPIE.**

Event: SPIE Astronomical Telescopes + Instrumentation, 2014, Montréal, Quebec, Canada

# Baseline design of the thermal blocking filters for the X-IFU detector on board ATHENA

M. Barbera<sup>\*a,b</sup>, A. Collura<sup>b</sup>, F. Gatti<sup>c</sup>, U. Lo Cicero<sup>b</sup>, C. Macculi<sup>d</sup>, L. Piro<sup>d</sup>, E. Renotte<sup>e</sup>, S. Sciortino<sup>b</sup>

<sup>a\*</sup>Università degli Studi di Palermo, Dipartimento di Fisica e Chimica, Via Archirafi 36, 90123 Palermo, Italy; <sup>b</sup>Istituto Nazionale di Astrofisica, Osservatorio Astronomico di Palermo, Piazza del Parlamento 1, 90134 Palermo, Italy; <sup>c</sup>Università di Genova, Dipartimento di Fisica, Via Dodecaneso 33, 16146 Genova, Italy; <sup>d</sup>Istituto Nazionale di Astrofisica, Istituto di Astrofisica e Planetologia Spaziale Roma, Via del Fosso del Cavaliere 100, 00133 Roma, Italy; <sup>e</sup>Centre Spatial de Liège, University of Liege, Liege Science Park, Avenue du Prè-Aily, 4031 Angleur, Belgium

## ABSTRACT

ATHENA is an advanced X-ray observatory designed by a large European consortium to address the science theme "Hot and Energetic Universe" recently selected by ESA for L2 – the second Large-class mission within the Cosmic Vision science program (launch scheduled in 2028). One of the key instruments of the mission is the X-ray Integral Field Unit (X-IFU), an array of Transition Edge Sensor (TES) micro-calorimeters with high energy resolution (2.5 eV @ 6 keV) in the energy range 0.2–12 keV, operating at the focal plane of a large effective area high angular resolution (5" HEW) grazing incidence X-ray telescope.

The X-IFU operates at temperatures below 100 mK and thus requires a sophisticated cryostat. In order to allow the beam focused by the telescope to reach the X-IFU detector, windows need to be opened on the cryostat thermal and structural shields surrounding the cold stage. X-ray transparent thermal blocking filters need to be mounted on such open windows to make the radiation heat-load onto the detector array negligible with respect to conduction heat load and dissipated electrical power, and to minimize photon shot noise onto the detector.

After a brief survey of the heritage from space satellite and sounding rocket experiments on thermal filters operated at cryogenic temperatures, we present the selected baseline design of the thermal filters for the ATHENA X-IFU detector, show the performances, and finally discuss possible improvements in the design to increase the X-IFU quantum efficiency at low energies.

**Keywords:** X-rays, missions, ATHENA, X-IFU, micro-calorimeter, Optical Blocking Filters

## 1. INTRODUCTION

ATHENA is an X-ray observatory-class mission [1] designed by a large European consortium to address the "Hot and Energetic Universe" science theme [2] selected by the European Space Agency for L2 – the second Large-class mission within the Cosmic Vision science program scheduled for launch in 2028.

Thanks to the innovative technology of its optics [3] and the most advanced focal plane X-ray instrumentation, the ATHENA mission will deliver X-ray (0.2-12 keV) wide field imaging, timing and high energy resolution spectroscopy capabilities far beyond those of any existing or approved future missions.

---

\* marco.barbera@unipa.it

One of the two detectors that will alternatively be mounted at the focal plane of the large area telescope of ATHENA is the X-ray Integral Field Unit (X-IFU) [4], an array of TES micro-calorimeters operating at temperatures below 100 mK, providing high spectral resolution ( $\Delta E_{\text{FWHM}} = 2.5 \text{ eV}$  at  $E < 7 \text{ keV}$ ) and imaging capabilities over a 5' diameter field of view [6].

In order to allow the X-ray beam focused by the large area telescope of ATHENA to reach the array of micro-calorimeters at the focal plane, a clear path has to be opened in the cryostat thermal and structural shields surrounding the cold stage[6], identified as the aperture cylinder. Optical blocking filters (OBF) need to be mounted on such shields to reduce the radiation heat-load from warmer surfaces onto the detector array. The micro-calorimeters operating as thermal detectors are also sensitive to photons at lower energies than X-rays. Although the detector does not trigger on individual low energy photons, the statistical fluctuation of the absorbed energy during the effective X-rays detection time, can introduce a degradation of the energy resolution of the detector known as shot noise. The OBF need to prevent the shot noise due to out of band radiation from the cryostat to deteriorate the intrinsic energy resolution of the micro-calorimeter detector. The OBF also significantly reduce the out of band radiation from target sources and background in the telescope field of view, however, particularly bright sources in the UV/VIS/IR (e.g. massive O stars, planets, QSO's, etc.) may need the use of additional optical filters in the filter wheel which will be mounted at the entrance of the cryostat aperture cylinder.

The use of filters to protect X-ray detectors for astrophysical observations is not a special requirement of low temperature detectors, in fact, any X-ray detector in space need to be protected by out of band radiation and/or low energy charged particles, and/or contamination. Thin plastic foils coated with a metal film or mesh supported metal films have been traditionally used for these purposes, allowing to get adequate out of band rejection and charge particle shielding at the price of an attenuation of soft X-rays. Large size filters with sub-micron thickness polyimide film coated with aluminum have been used in many recent missions such as Chandra[7][8], and XMM-Newton [9], demonstrating reliability and long-term stability. Polyimide is quite robust and can be used unsupported even for quite large diameter filters; as an example, the thin filters of the EPIC camera on board XMM-Newton are nearly 75 mm diameter and consist of an unsupported 1200 Å thick Polyimide film with a 400 Å thick aluminum layer. Such filters have survived launch and are still working with no clear sign of degradation [10][11].

A few experiments have been flown in the past with doped-silicon sensor X-ray micro-calorimeter detectors operating at low temperatures. Such detectors, like the X-IFU, needed to be protected from radiation power from the cryostat outer shields. In the X-ray Quantum Calorimeter Sounding Rocket Program, a joint effort between the University of Wisconsin and Goddard Space Flight Center to resolve the spectrum of the soft X-ray background using an array of very sensitive micro-calorimeters [12], different solutions have been adopted since the first launch in 1996. The first OBF design consisted of four free standing 1000 Å thick parylene films coated with 200 Å of aluminum [12]. In the most recent launches of 2008, 2011 and 2014 the OBF have been built using aluminum coated polyimide either unsupported or supported by a highly transparent Si mesh for the outer and larger diameter filters [13]. The Si mesh is obtained by Deep Reactive Ion Etching of a Si wafer, and thanks to the good thermal conductivity of Si, heaters mounted on the backing ring allow to warm-up the filters for contamination de-icing. The Si meshes are quite brittle and thus they cannot be rigidly tightened to a metal supporting ring. For this reason, they are attached on a kinematic mount which has the disadvantage of not being leak tight, thus requiring the use of a moisture shield to minimize contamination of the inner shields. The aluminum coated polyimide film was deposited onto the Si meshes by LUXEL corp.

The ASTRO-E and ASTRO-E2 (Suzaku) X-ray observatory missions launched in 2000 and 2005 carried on board a small array of micro-calorimeter detectors. For these missions the combination of polyimide and aluminum was adopted for the OBF, with a supporting Ni mesh for the larger diameter filters [14][15]. The Micro-X sounding rocket experiment under development at the Massachusetts Institute of Technology will use a transition-edge-sensor X-ray-micro-calorimeter array with a conical imaging mirror to obtain high spectral-resolution images of extended X-ray sources [16]. The OBF design is the same as that one adopted for the last launches of the Quantum Calorimeter Sounding Rocket Experiment [17]. The Japanese ASTRO-H high-energy observatory mission, scheduled for launch in 2015, will carry on board an X-ray micro-calorimeter array with doped-silicon sensors [18]. The three outer OBF consist of a Polyimide film 1000 Å thick coated with 800 Å of aluminum supported by a 96% open area Si mesh (diameters 35 mm, 24 mm, and 18.5 mm, respectively). The two inner OBF with a diameter of 12 mm are free standing and consist of a Polyimide film 800 Å thick coated with 800 Å of aluminum [19][20].

## 2. OBF BASELINE DESIGN

The radiation load from hot surfaces in the temperatures range between 2 K and 300 K is mainly in the IR region with wavelength between 1  $\mu\text{m}$  and few cm. In this region aluminum presents a very high reflectivity and quite good absorption as well. The left panel in Figure 1 shows a simulated reflection curve for 100  $\text{\AA}$ , 200  $\text{\AA}$ , 300  $\text{\AA}$  and 400  $\text{\AA}$  thick aluminum films. The right panel of Figure 1 shows the transmission curves for the same films. The calculations are derived by the use of the matrix formulation of the boundary conditions of the electromagnetic field [21], with the refractive index of aluminum derived from three different sources for the wavelength range 0.01653  $\div$  32  $\mu\text{m}$  [22], 33.333  $\div$  200  $\mu\text{m}$  [23], and 248  $\div$  1240  $\mu\text{m}$  [24], respectively.

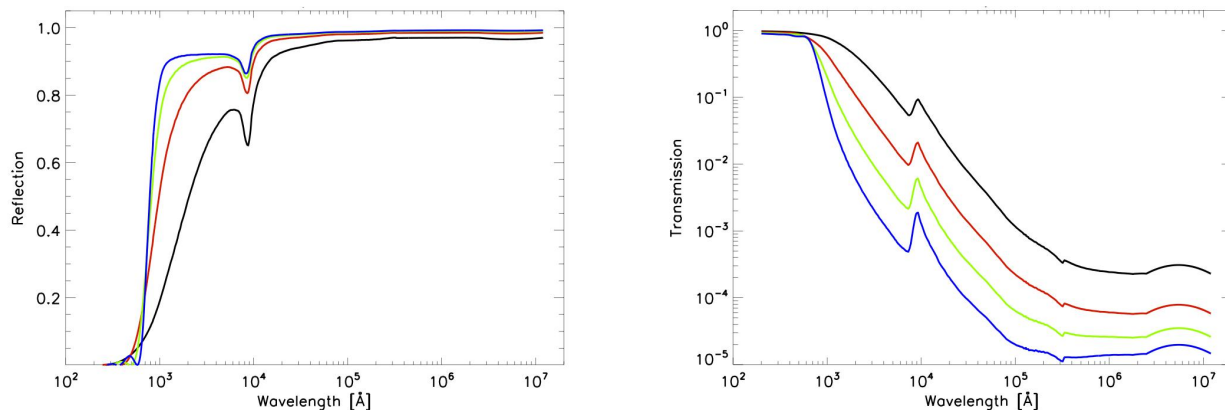


**Figure 1.** Calculated reflection of a single layer of aluminum 100  $\text{\AA}$  (black), 200  $\text{\AA}$  (red), 300  $\text{\AA}$  (green) and 400  $\text{\AA}$  thick (blue), respectively (left panel). Calculated transmission of the same layers of aluminum (right panel).

As it is evident from the left panel, a layer of aluminum 100  $\text{\AA}$  thick provides already a reflectivity larger than 95% in the IR region of thermal radiation at  $T < 300$  K. The transmission (right panel) changes by slightly more than an order of magnitude by changing the aluminum layer thickness by a factor four, confirming that reflection plays the main role in blocking the IR radiation. The aluminum reflectivity marginally changes in the IR for thicknesses larger than 200  $\text{\AA}$ . On the other hand, aluminum is oxidized both on the open face and on the interface with polyimide [25][26]. In the past, we have estimated an oxidation layer of the order of 50  $\text{\AA}$  on each side of the aluminum layer coated on a polyimide film, both by UV/Vis transmission measurements, and more recently by X-ray photoelectron spectroscopy measurements conducted on samples of the XMM-Newton EPIC camera thin and medium filters [27][28]. As a first approximation the aluminum oxide layer becomes nearly transparent and thus only the effective bulk aluminum layer has to be considered in designing the filter and in calculating the optical blocking factor.

Polyimide is quite transparent in the visible and near IR while it strongly absorbs radiation in the UV at wavelengths shorter than about 3500  $\text{\AA}$ [7]. In the far IR molecular absorption bands occur at wavelengths larger than approximately 20000  $\text{\AA}$  that may significantly reduce the transmission [29][30]. For our purposes of designing an optical blocking filter we can conservatively consider polyimide to be nearly transparent at wavelength larger than 20000  $\text{\AA}$ . Figure 2 shows a plot of calculated transmission for a 1000  $\text{\AA}$  film of polyimide based on the refractive index reported by Cavadi et al. 2001[31]. This refractive index was calculated upon transmission measurements performed on Hitachi PIQL-100 polyimide samples provided by LUXEL corp., which is the same material used for the filters of the Chandra HRC [8].

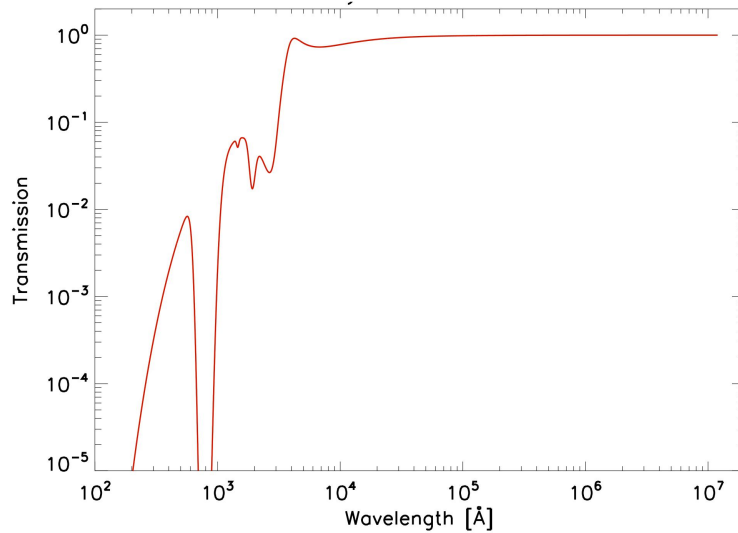


**Figure 2.** Calculated transmission of a single layer of polyimide 1000 Å thick.

Despite the adopted approximation it is clear that aluminum blocks the IR thermal radiation while polyimide essentially plays the role of a mechanical support for the aluminum and provides absorption to out of band radiation in the UV band.

The baseline design of the OBF for the X-IFU experiment, which is largely based on the investigation conducted during the IXO-XMS study phase and ASTRO-H development [32][33], consists of 5 identical filters for a total of 2800 Å of polyimide and 2100 Å of aluminum, with the two outer and larger diameter filters supported by a 10 μm thick integrated polyimide grid (93 % open area). Figure 3 shows a plot of the transmission of a single filter (left panel) and of the integrated set of five filters (right panel). Superimposed in the plots are the wavelengths of the peak thermal emission from the cryostat shields. Notice that despite each filter has 420 Å of aluminum, the plotted transmission considers only 320 Å of aluminum per filter assuming that a layer of 100 Å has been oxidized and becomes nearly transparent.

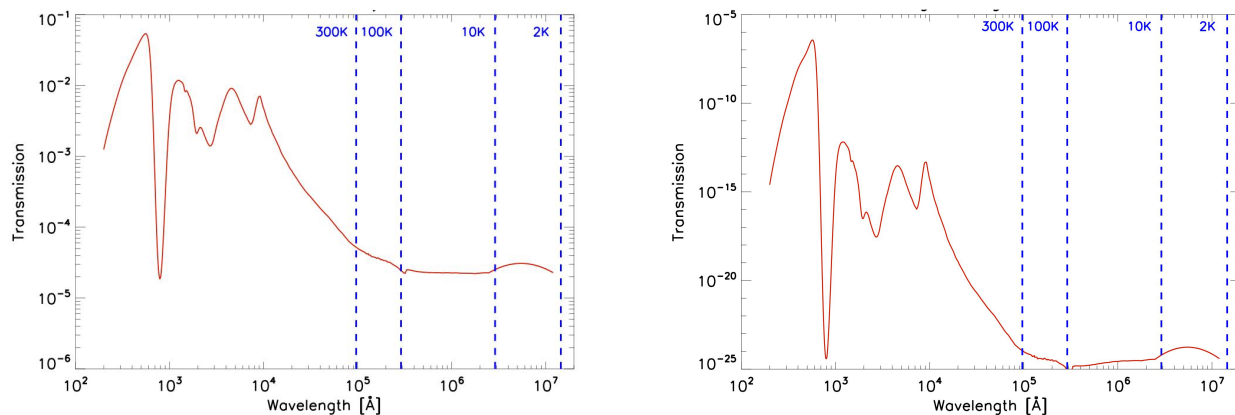


**Figure 3.** Calculated transmission of a single optical blocking filter consisting of 560 Å polyimide and 320 Å aluminum (left panel). Calculated total transmission for the full set of five filters (right panel).

In order to calculate the efficiency of the baseline OBF design in reducing the thermal radiation load below the available cooling power at the cold stage, as well as in limiting the shot noise onto the micro-calorimeter detectors, we have adopted the schematic shown in Figure 4. This scheme is not necessary consistent with the final design of the X-IFU

aperture cylinder and cryostat, however it is a realistic case based on the current study phase, and will be updated during the ATHENA mission development phase. Given the ATHENA large area telescope geometry (diameter = 3 m, F.L. = 12 m), the filter diameters are constrained by the adopted filter distances from the detector array .

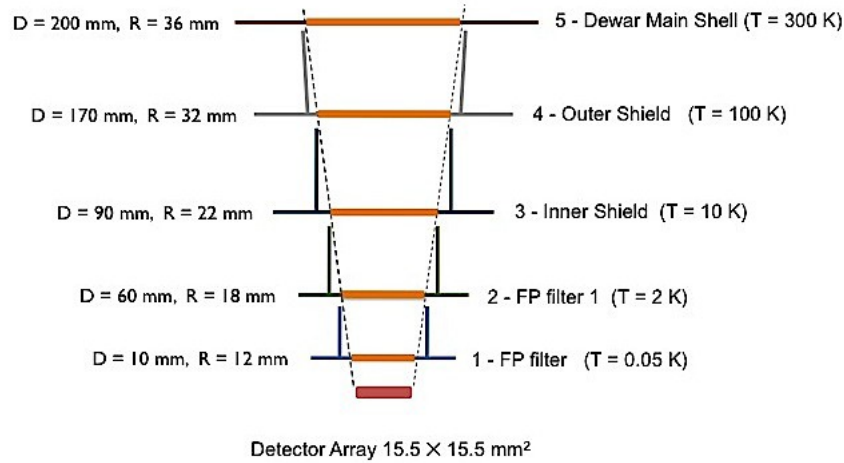


**Figure 4.** Adopted scheme for the optical blocking filters in the cryostat aperture cylinder. The filter temperatures, distances from the detector array (D), and radii (R) are shown in the schematic drawing.

In order to calculate the total power irradiated onto the detector array we have done the following further assumptions:

1. each filter behaves as an ideal black body radiation source (conservative assumption);
2. filters are tilted by  $5^\circ$ , in alternate directions, with respect to the horizontal plane, to reduce multiple reflections;
3. the micro-calorimeter detection time is 1 ms (conservative assumption);
4. the detector array size is  $15.5 \times 15.5 \text{ mm}^2$ , and consists of 3844 square pixels each one  $250 \times 250 \text{ }\mu\text{m}^2$ ;

The following expressions have been used to calculate the energy resolution degradation due to shot noise:

$$NEP^2(T) = \frac{1}{n\_pixels} \int_{\lambda_{min}}^{\lambda_{max}} 2 \cdot P(\lambda, T) \cdot \frac{hc}{\lambda} \cdot d\lambda \quad [\text{W}\cdot\text{J}] ;$$

$$\Delta E_{FWHM} = 2.35 \cdot 6.2415 \cdot 10^{+18} \cdot \sqrt{NEP^2(T) \cdot \tau_{det}} \quad [\text{eV}] ;$$

where  $P(\lambda, T)$  is the total power spectral density ( $\text{W}/\text{\AA}$ ) arriving onto the detector array from the shield at temperature  $T$ ,  $h$  is the Planck constant,  $c$  is the speed of light,  $n\_pixels$  is the total number of pixels in the array, and  $\tau_{det}$  is the micro-calorimeter detection time. Figure 5 shows the calculated radiation load onto the full detector array, while Table 1 reports the filter characteristics, the integrated power on the array irradiated from each shield, the energy resolution degradation due to the thermal radiation from each shield and the average number of reflection in the interface between each filter and the inner one.

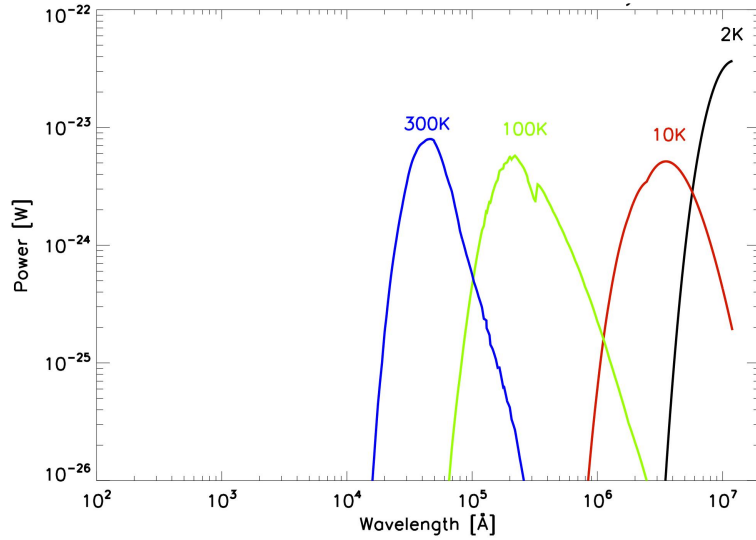


**Figure 5.** Radiation load onto the detector array from each of the warm shields of the cryostat aperture cylinder based on the use of the baseline design OBF.

**Table 1.** The table reports for each filter, its temperature (T), distance from the detector array (D), radius (R), integrated radiation power onto the detector array, contribution to the energy resolution degradation by shot noise ( $\Delta E_{FWHM}$ ), and average number of reflection in the interface between each filter and the inner one ( $N_{REFL}$ ).

	T [K]	D [mm]	R [mm]	Power [ $10^{-19}$ W]	$\Delta E_{FWHM}$ [eV]	$N_{REFL}$
OBF1	0.050	10	12			
OBF2	2	60	18	1409.85	0.0018	2
OBF3	10	90	22	225.46	0.0011	4
OBF4	100	170	32	16.59	0.0011	2
OBF5	300	200	36	3.01	0.0012	4
<b>Total</b>				<b>1654.91</b>	<b>0.0027</b>	

As it can be inferred from Table 1, the baseline design of the OBF for the X-IFU detector is quite conservative given the present adopted parameters for the aperture cylinder and cryostat. The total radiation power onto the detector array is many orders of magnitude lower than the available cooling power at the cold stage which is presently estimated to be between 1 and 2  $\mu$ W, and the energy resolution degradation due to shot noise is three orders of magnitude lower than the intrinsic detector energy resolution. The calculations can be improved with more refined calculations including some radiation contributions and multiple reflections from the lateral walls of the aperture cylinder, however, we expect this to introduce small corrections to the presented results. On the other hand the calculation is quite conservative in considering the OBF as an ideal black body source; in fact, shining aluminum can have an emissivity coefficient as low as 0.01, thus significantly reducing the emitted radiation power.

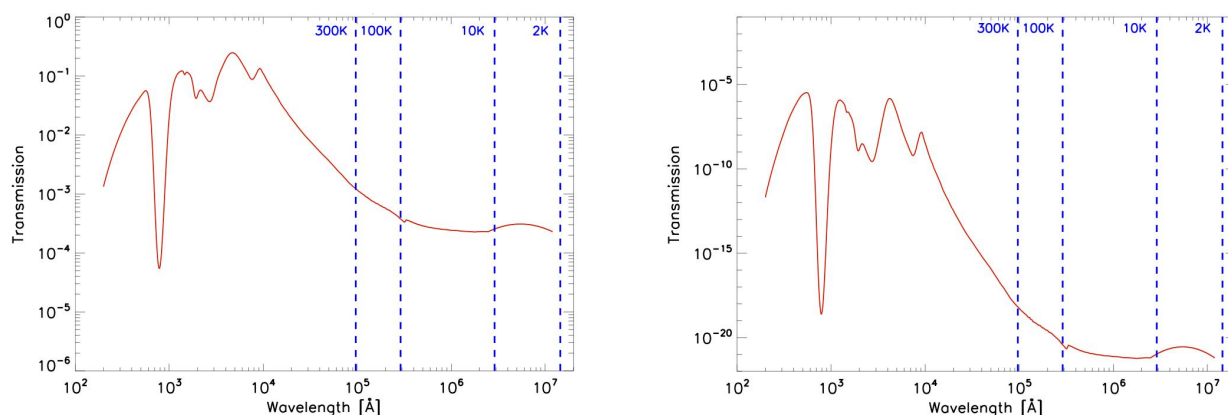
### 3. DESIGN OPTIMIZATION

Some of the key science goals of the ATHENA mission require  $2 \text{ m}^2$  effective area at 1 keV and a low energy threshold response lower than 0.2 keV. A few of these science goal are: the search for missing baryons in the Universe; the study of the interaction of AGN winds and star-bursts with their galaxy environment; the census of the high Z AGN's; the search for the first generation of stars, the formation of the first black holes, and the dissemination of the first metals in the Universe. A more extensive description of the ATHENA science goals and associated requirement for low energy response are presented in the proposal submitted to ESA in April 2014 in response to the call for an L class mission in the Hot and Energetic Universe theme due for launch in 2028[1][2].

The effective area at 1 keV of the X-ray Integral Field Unit and the low energy threshold response largely depend on the transmission of the aperture cylinder OBF. The present baseline design of the OBF presented in the previous section, while being adequate to fulfill the requirements on radiation heat load and shot noise, is not fully optimized to maximize the low energy response of the X-IFU.

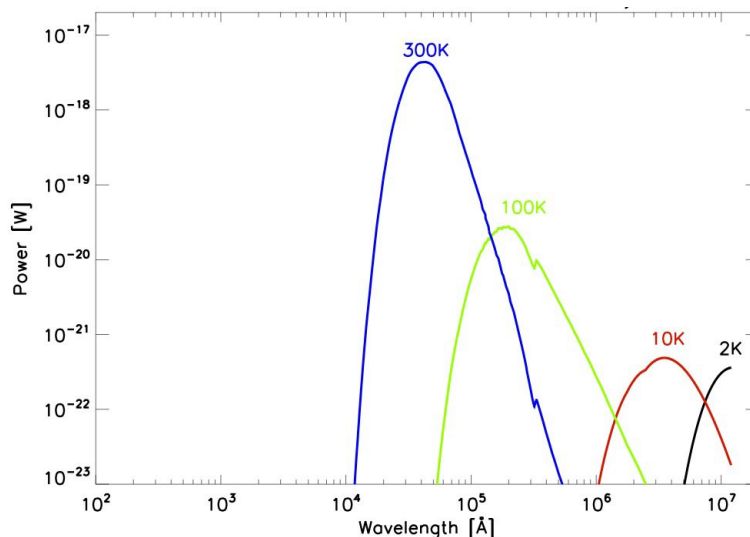
The use of the modeling developed to calculate the radiation load onto the detector array gives us a useful tool to optimize the optical design of the OBF before coming into the investigation of technical issues such as mechanical robustness to withstand launch stresses, need for heaters to run de-icing procedures to remove contaminations, type of meshes, if needed, to support the larger diameter filters, inner carbon coating to reduce multiple reflection, etc. In this section as a case study we will evaluate the optical performance of a more transparent OBF design, aimed at increasing the low energy response, consisting of 5 identical filters with a total of 2250 Å of polyimide and 1000 Å of aluminum, with a mesh with 97% open area, similar to the one adopted for ASTRO-H, to mechanically support the two larger diameter filters.

Figure 6 shows a plot of the transmission of a single filter (left panel) and of the integrated set of five filters (right panel). Superimposed in the plots are the wavelengths of the peak thermal emission from the cryostat shields. As in the previous case the plotted transmission assumes that a layer of 100 Å has been oxidized and becomes nearly transparent.



**Figure 6.** Calculated transmission for a single optical blocking filter consisting of 450 Å of polyimide and 100 Å of aluminum (left panel). Calculated total transmission for the full set of five filters (right panel).

Figure 7 and Table 2 show the results of the calculations performed on this new set of filters as previously done for the baseline design.



**Figure 7.** Irradiated power onto the detector array from the warm shields of the cryostat aperture cylinder based on the use of a new set of OBF with a thinner layer of aluminum and polyimide to improve the X-IFU low energy response.

**Table 2.** Same calculations as in Table 1 but for the new set of OBF with a thinner layer of aluminum and polyimide to improve the X-IFU low energy response.

	T [K]	D [mm]	R [mm]	Power [ $10^{-16}$ W]	$\Delta E_{FWHM}$ [eV]	$N_{REFL}$
OBF1	0.050	10	12			
OBF2	2	60	18	13.83	0.0057	2
OBF3	10	90	22	21.36	0.011	4
OBF4	100	170	32	57.93	0.076	2
OBF5	300	200	36	1536.85	0.87	4
<b>Total</b>				<b>1629.97</b>	<b>0.87</b>	

The radiation power onto the detector array is still many orders of magnitude lower than the available cooling power, on the other hand the energy resolution degradation due to shot noise has become a significant fraction of the intrinsic energy resolution of the detector. Given the conservative assumptions we have done considering the filters as an ideal black body radiation sources, and using a quite long detection time of 1 ms, it is likely that a more accurate estimate which takes into account the emissivity of aluminum and a shorter detection time would already reduce this number to an acceptable value.

Figure 8 shows a comparison of X-ray transmission in the energy range of sensitivity of Athena for the ASTRO-H XRS OBF set, the X-IFU OBF baseline design, and the X-IFU OBF case study design aimed at obtaining a larger effective area in the soft X-rays. The X-IFU baseline OBF is already more efficient than the ASTRO-H XRS filters, however, the comparison with the case study OBF suggests that an optimization of the OBF design can provide a significant further improvement in low energy response.

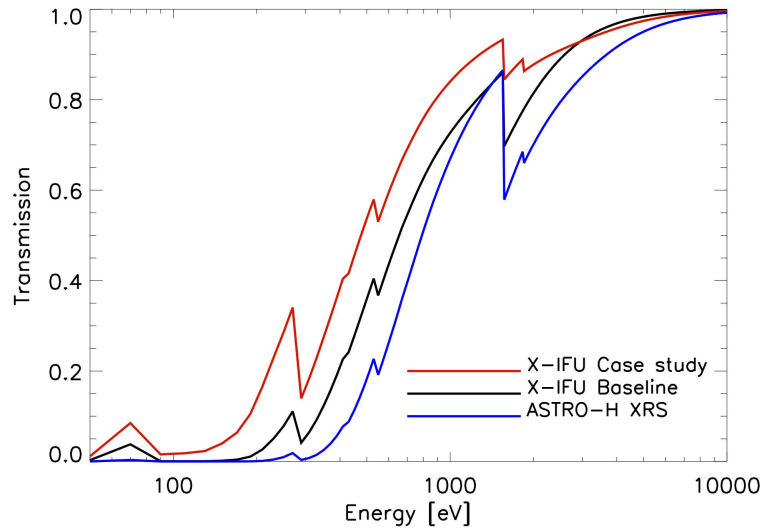


**Figure 8.** Comparison of X-ray transmission in the energy range of sensitivity of Athena for the ASTRO-H XRS OBF set, the X-IFU OBF baseline design, and the X-IFU OBF case study design aimed at obtaining a larger effective area in the soft X-rays.

#### 4. SUMMARY AND CONCLUSIONS

In this paper we have presented some preliminary results on the optical performances of the optical blocking filters needed to protect the X-IFU X-ray micro-calorimeter detector array from the thermal radiation of the cryostat shields. Based on the large successful experience with thin aluminized polyimide films used in different space missions over the last two decades to protect mirrors and detectors from out of band radiation and low energy particles, we suggest to use these materials also for the X-IFU OBF. Unsupported large area thin films of polyimide with similar diameters to the X-IFU OBF have been flown in previous missions such as XMM-Newton. However, the polyimide thickness for the X-IFU OBF is more than a factor two smaller than that one used on the XMM-Newton EPIC camera, therefore the use of a supporting mesh for the outer and larger diameter filters has to be considered.

Aluminum blocks, mainly by reflection, the thermal IR radiation from the cryostat shields. There is no significant gain in reflection by increasing the aluminum thickness above 200 Å. On the other hand, aluminum is known to develop an aluminum oxide layer of about 50 Å both on the open surface and on the interface with polyimide. As a first approximation the aluminum oxide is transparent and therefore the choice of the aluminum thickness has to take this effect into account. Polyimide is nearly transparent in the VIS/IR while it absorbs the UV at wavelengths lower than 3500 Å, and provides the mechanical support to aluminum.

The baseline design of the X-IFU OBF, largely based on the investigation carried out during the study phase of the IXO-XMS experiment and Astro-H, consists of a set of 5 identical filters for a total of 2800 Å of polyimide and 2100 Å of aluminum. A thick integrated polyimide supporting mesh with 93% open area is taken into account for the two outer and larger diameter filters.

In order to estimate the optical performance of the OBF we have adopted a preliminary design of the aperture cylinder and cryostat shield temperatures. The results obtained by the modeling shows that the baseline design fully satisfy the requirement on optical load and shot noise even if we assume that a layer of aluminum 100 Å thick becomes transparent on each filter because of oxidation.

Given the strong request from the Athena science cases to increase the low energy response of the X-IFU, we have also considered, as a case study, a more transparent OBF design consisting of five identical filters with a total of 2250 Å of

polyimide and 1000 Å of aluminum, with a 97% open area mesh to mechanically support the two larger diameter filters. The results of the calculations for this new set of filters show again a safe condition in terms of radiation power onto the array, while the shot noise turns out to be about 0.8 eV, and thus not negligible with respect to the intrinsic energy resolution of the detectors. It is likely that a more refined modeling, which takes into account the emissivity coefficient of aluminum either than treating it as an ideal black body, would reduce also the shot noise making this design compatible with the scientific requirements. The case study OBF design allows to obtain a significant improvement in effective area at low energy.

In this paper we have not presented any discussion on the technical feasibility of such filters from the mechanical robustness point of view, neither have we discussed any details on the design of the filter frames, mounting approach on the aperture cylinder, type of supporting meshes if needed on the outer shields, need for heaters for de-icing procedures, nor we have investigated issues related to the reduced thermal and electrical conductivity of aluminum layers at sub micron thickness. These subjects of investigation and design will be part of the X-IFU technology development activities that should start in 2015.

### ACKNOWLEDGEMENTS

We acknowledge fruitful suggestions and advice by prof. Dan McCammon. We acknowledge partial support by the Italian Space Agency, and EU under the project CESAR (FP7-SPACE-2010-1, Project no. 263455).

### REFERENCES

- [1] Nandra K., Barret D., Barcons X., Fabian A.C., den Herder J.W. A., Piro L., Watson M. G., "Athena: exploring the hot and energetic universe", Proc. SPIE, this conference, paper 9144-84 (2014).
- [2] Nandra, K., Barret, D., Barcons, X., Fabian, A., den Herder, J.-W., Piro, L., Watson, M., Adami, C., Aird, J., Afonso, J. M., and et al., "The Hot and Energetic Universe: A White Paper presenting the science theme motivating the Athena+ mission" 2013arXiv1306.2307N (June 2013).
- [3] Willingale, R., Pareschi, G., Christensen, F., and den Herder, J.-W., "The Hot and Energetic Universe: The Optical Design of the Athena+ Mirror" 2013arXiv1307.1709W (July 2013).
- [4] Ravera L., Barret D., den Herder J.W., Piro L., Cledassou R., Pointecouteau E., Philippe Peille, Pajot F., Arnaud M., Pigot C., Duband L., Cara C., den Hartog R.H., Gottardi L., Akamatsu H., van der Kuur J., van Weers H.J., de Plaac J., Macculi C., Lotti S., Torrioli G., Gatti F., Valenziano L., Barbera M., Barcons X., Ceballos M.T., Fabrega L., Mas-Hesse J.M., Page M.J., Guttridge P.R., Willingale R., Fraser G.W., Paltani S., Genolet L., Bozzo E., Rauw G., Renotte E., Wilms J., and Schmidt C., "The X-ray Integral Field Unit (X-IFU) for Athena", Proc. SPIE, this conference, paper 9144-92 (2014).
- [5] Gottardi, L., Akamatsu, H., Barret, D., Bruin, M. P., den Hartog, R. H., den Herder, J.-W. A., Hoevers, H. F., van der Kuur, J., Jambunathan, M., and Ridder, M. L., "Development of TES-based detectors array for the x-ray integral field unit (X-IFU) on the future x-ray observatory Athena", in this proceeding , paper 9144-93 (2014).
- [6] van Weers, H. J., den Herder, J.-W. A., Jackson, B. D., and Kooijman, P. P., "Tes-detector based focal plane assembly key-technology developments for ATHENA and SAFARI", Proc. SPIE, this conference, paper 9144-225 (2014).
- [7] Barbera M, Austin K, Collura A, Flanagan A, Jelinsky R, Murray S, Serio S, Zombeck M, "Development of the UV/ion shields for the Advanced X-ray Astrophysics Facility high-resolution camera (AXAF HRC)", PROC. SPIE, vol. 2280, p. 214-228 (1994).
- [8] Meehan R, Murray S, Zombeck V, Kraft P, Kobayashi K, Chappell H, Kenter T, Barbera M, Collura A, Serio S, "Calibration of the UV/ion shields for the AXAF High-Resolution Camera", PROC. SPIE, vol. 3114, p. 74-100 (1997).
- [9] Villa GE, Barbera M, Collura A, La Palombara N, Musso C, Serio S, Stillwell R, Tognon P, Turner DC The optical/UV filters for the EPIC experiment. IEEE Transactions on Nuclear Science, vol. 45, p. 921-926 (1998), doi: 10.1109/23.682670
- [10] Barbera M, Agnello S, Buscarino G, Collura A, Gastaldello F, La Palombara N, Lo Cicero U, Tiengo A, Sciortino L, Varisco S, Venezia A M, "Status of the EPIC thin and medium filters on-board XMM-Newton after more than 10 years of operation: 1) laboratory measurements on back-up filters", PROC. SPIE, 8859, 14, 1-12

- (2013).
- [11] Gastaldello F, Barbera M, Collura A, La Palombara N, Lo Cicero U, Sartore N, Tiengo A, Varisco S, "Status of the EPIC thin and medium filters on-board XMM-Newton after more than 10 years of operation: 2) analysis of in-flight data", *PROC. SPIE*, 8859, 15, 1-6 (2013).
  - [12] McCammon D., et al, "A sounding rocket payload for X-Ray Astronomy employing high resolution microcalorimeters", *Nucl. Instrum. Methods A* 370, 266 (1996)
  - [13] McCammon D., et al., "The X-ray Quantum Calorimeter Sounding Rocket Experiment: Improvements for the Next Flight", *JLTP*, 151, Issue 3-4, pp 715-720 (2008).
  - [14] Audley, M.D., et al., "ASTRO-E/XRS blocking-filter calibration", *Proc. SPIE Vol. 3765*, p. 751-761 (1999).
  - [15] Kelley, R.L., Mitsuda, K., Allen, C.A., et al., "The Suzaku High Resolution X-Ray Spectrometer", *PASJ* **59**, 77-112 (2007).
  - [16] Wikus, P. et al., "Progress on the Micro-X sounding rocket x-ray telescope: completion of flight hardware", *Proc. SPIE*, 7732, 1P, p. 1-15 (2010).
  - [17] Figueroa-Feliciano, E.; Adams, J. S.; Baker, R.; Bandler, S. R.; Dewey, D.; Doriese, W. B.; Eckart, M. E.; Hamersma, R.; Hilton, G. C.; Hwang, U.; Irwin, K. D.; Kelley, R. L.; Kilbourne, C. A.; Kissel, S. E.; Leman, S. W.; McCammon, D.; Oakley, P. H. H.; Okajima, T.; O'Neal, R. H.; Petre, R.; Porter, F. S.; Reintsema, C. D.; Rutherford, J. M.; Saab, T.; Serlemitsos, P.; Soong, Y.; Trowbridge, S. N.; Wikus, P., "Update on the Micro-X Sounding Rocket payload", *Proc. SPIE*, Vol. 8443, 1B, p. 1-17 (2012).
  - [18] Mitsuda, K. et al., "The X-ray microcalorimeter on the NeXT mission", *Proc. SPIE*, 7011, 2K, p. 1-8 (2008).
  - [19] de Vries, C.P., et al., "Filters and calibration sources for the soft x-ray spectrometer (SXS) instrument on ASTRO-H", *Proc. SPIE*, 7732, 13, p. 1-9 (2010).
  - [20] Takahashi, T. et al., "The ASTRO-H Mission", *Proc. SPIE*, 7732, 0Z, p.1-18 (2010).
  - [21] Born M. and Wolf E., "Principles of Optics", 6th edition (1997), Cambridge University Press (UK), ISBN 0521639212.
  - [22] D.Y. Smith, "The optical properties of metallic aluminum", in *Handbook of Optical Constants of Solids*, p. 369-406 (1985), Edited by Edward D. Palik, ISBN: 978-0-12-544415-6
  - [23] Aleksandar D. Rakic., "Algorithm for the determination of intrinsic optical constants of metal films: application to aluminum", *Appl. Opt.* 34, 4755-4767 (1995)
  - [24] H.-J. Hagemann et al., "Optical constants from the far infrared to the x-ray region: Mg, Al, Cu, Ag, Au, Bi, C, and Al<sub>2</sub>O<sub>3</sub>", *J. Opt. Soc. Am.* 65, 742-744 (1975).
  - [25] J. J. Pireaux, M. Vermeersch, C. Grégoire, P. A. Thiry, R. Caudano and T. C. Clarke, "The aluminum-polyimide interface: An electron-induced vibrational spectroscopy approach", *J. Chem. Phys.* 88, 3353 (1988); <http://dx.doi.org/10.1063/1.453930>.
  - [26] M. J. Vasilel and B. J. Bachman, "Aluminum deposition on polyimides: The effect of in situ ion bombardment", *J. Vac. Sci. Technol. A* 7, 2992 (1989); <http://dx.doi.org/10.1116/1.576305>
  - [27] Barbera M, Collura A, Artale A, Varisco S, Peres G, Sciortino S, Serio S, Villa G E. Monitoring the stability of thin and medium back-up filters of the Newton-XMM EPIC camera, *PROC. SPIE*, vol. 4851, p. 264-269 (2003), doi: 10.1117/12.461592
  - [28] Barbera M, Agnello S, Buscarino G, Collura A, Gastaldello F, La Palombara N, Lo Cicero U, Tiengo A, Sciortino L, Varisco S, Venezia A M. Status of the EPIC thin and medium filters on-board XMM-Newton after more than 10 years of operation: 1) laboratory measurements on back-up filters. *PROC. SPIE*, 8859, 14, 1-12 (2013).
  - [29] Zhang Z.M., Lefever-Button G., and Powell F.R., "Infrared refractive index and extinction coefficient of polyimide films", *International Journal of Thermophysics*, vol. 19, N. 3, p. 905-916 (1998).
  - [30] Kawka P.A. and Buckius R.O., "Optical properties of Polyimide films in the Infrared", *International Journal of Thermophysics*, vol. 22, N. 2, 517-534 (2001).
  - [31] Cavadi A, Artale A, Barbera M, Collura A, Powell R, Varisco S, "Measurement of optical constants n and k of lexan and polyimide", *PROC. SPIE*, vol. 3765, p. 805-815 (1999).
  - [32] Mitsuda K., et al., "Soft x-ray spectrometer (SXS): the high-resolution cryogenic spectrometer onboard ASTRO-H", *Proc. SPIE*, this conference, paper 9144-81 (2014).
  - [33] M.A. Leutenegger, G.V. Brown, S.E. Busch, M.E. Eckart, N.H. Friedrich-Alexander, R.L. Kelley, C.A. Kilbourne, D. McCammon, J.P. Porst, F. S. Porter, "X-ray transmission of the Astro-H soft x-ray spectrometer optical blocking filters", *Proc. SPIE*, this conference, paper 9144-208 (2014).